

PAPER • OPEN ACCESS

An Alternative Solution for Microfluidic Chip Fabrication

To cite this article: C Ongaro *et al* 2022 *J. Phys.: Conf. Ser.* **2385** 012029

View the [article online](#) for updates and enhancements.

You may also like

- [Correlation between the metallization corrosion and acetic acid in crystalline silicon photovoltaic module](#)
Taeko Semba
- [Reduction in contact resistivity of Ag thick-film conductor on SiN_x-coated Si wafer for solar cell using lead tellurite glass frit](#)
Yusuke Tachibana, Akifumi Matsuda and Mamoru Yoshimoto
- [Corrosion mechanism analysis of the front-side metallization of a crystalline silicon PV module by a high-temperature and high-humidity test](#)
Taeko Semba



The Electrochemical Society
Advancing solid state & electrochemical science & technology

247th ECS Meeting
Montréal, Canada
May 18-22, 2025
Palais des Congrès de Montréal

Showcase your science!

Abstract submission deadline extended: December 20

ECS UNITED

The poster features a large graphic of a hand holding a globe with a stylized 'E' on it, set against a background of blue and green wavy patterns and a dotted grid.

An Alternative Solution for Microfluidic Chip Fabrication

C Ongaro¹, A Betti¹, B Zardin^{1,a}, V Siciliani², L Orazi², J Bertacchini^{3,4}, M Borghi¹

¹Engineering Department Enzo Ferrari DIEF, via P. Vivarelli 10, 41125 Modena Italy

²Department of Sciences and Methods for Engineering DISMI, via Amendola 2, Pad. Morselli, 42122 Reggio Emilia Italy

³Department of Surgery, Medicine, Dentistry and Morphological Sciences with Interest in Transplant, Oncology and Regenerative Medicine, CHIMOMO, via del Pozzo 71, 41125 Modena Italy

⁴Istituto di Genetica Molecolare "Luigi Luca Cavalli-Sforza", Consiglio Nazionale delle Ricerca (IGM-CNR), 40136 Bologna, Italy.

^abarbara.zardin@unimore.it

Abstract. This paper focuses on microfluidic devices, widely used in bioengineering. Their fabrication for research is almost entirely made of PDMS (a silicone), using photolithography and replica molding technologies, which involve many processing steps, sealed with a glass layer by plasma bonding. Our solution fabricates devices in just two steps, laser ablation of a glass layer, technology already extensively tested, and sealing with a commercial silicone layer by plasma bonding, drastically reducing skilled human operations and lead time. The paper describes the technologies with PDMS and with our solution, the design of a microfluidic test chip, the laser ablation and assessment by a confocal microscope of the microfluidic circuit in the glass layer of the chip, the plasma bonding of glass layers with PDMS and two other commercial silicones utilizing a grid of different plasma parameters, the qualitative assessment of the plasma bonding and choosing of a silicone as PDMS substitute, the extensive test on the bonding quality by two different pressure circuits on a batch of microfluidic chips realized with our proposed technology.

1. Introduction

The term microfluidics refers to the science and technology that manipulates small amounts of fluid between 10^{-6} to 10^{-12} liters within structures or channels that have dimensions in the micrometer scale or smaller, usually between 1 μm and 1 mm. The main technological application is the creation of "Lab-on-chips" (LOC), microfluidic-based systems that integrate multiple laboratory capabilities on a single chip only a few centimeters in size into which micrometer-sized channels are obtained or special scaffolds are used [1]. These devices are widely used in a variety of fields, from physics and biology to material one, but they have especially relevance in the biomedical field, for example, for 'amplification' of small DNA strands, dielectrophoresis, immunological testing, and others. The advantages of this technology over traditional testing are numerous. First, working with such small sample sizes allows the use of smaller amounts of chemicals and reagents and greater control over the motion of the fluids and their interaction. This translates into lower costs certainly but also improved safety, as it allows more containment and control of any toxic substances involved in the tests and more accurate results [2].

For decades, the technology to produce microfluidic circuits for biological research, and others, has been based on 'replica molding' where PDMS, a type of silicone, is cured on a mold which, through photolithography, reproduces in negative the circuit to be made. The circuit is sealed by 'plasma bonding' of a glass layer on the PDMS [3-5]. Figure 1 shows the main steps of this technology.

Several attempts were made to replace this technology but were not very successful due to less practicality than 'replica molding' [6-8]. For example, the microfluidic circuit was engraved on glass by 'laser ablation', a faster process than photolithography. The problem was that PDMS was always needed to seal the circuit, the curing of which takes a long time and many processing steps [9].

Particularly ultrashort pulsed lasers that remove material without significant heat transfer to surrounding areas [10] have been used to modify the glass surface to create microchannels with the desired geometry [11-14].



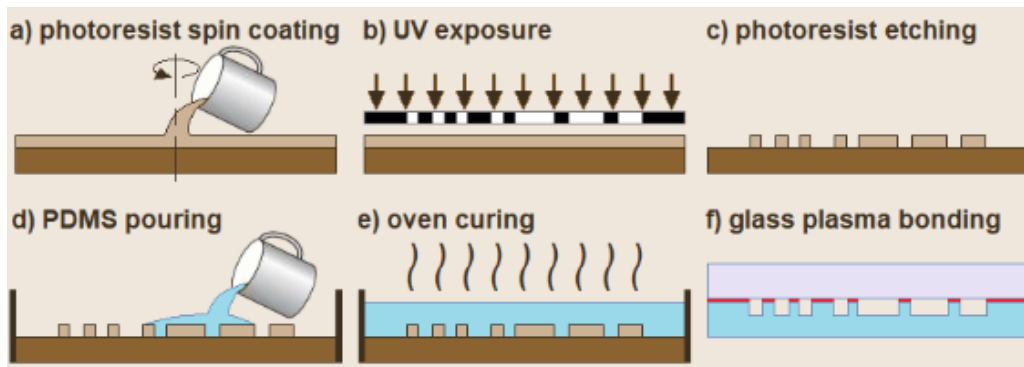


Figure 1. PDMS replica molding, adapted from [2].

In [11,13] a picosecond pulsed laser system is the only tool needed to fabricate a glass microfluidic device. The approach of performing an in-bulk process on the glass has also been followed [12] but machining the surface and then closing the channel is simpler and improves the geometric accuracy [14].

PDMS, and similar special silicones compatible with biological applications, are now available on the market in sheets of different thickness. This study aimed to test these materials for their use in microfluidic circuits, in glass sealing by ‘plasma bonding’, eliminating the long process of PDMS curing. Figure 2 shows the only two steps proposed by this paper: rapid and precise laser ablation and sealing by plasma bonding. One challenge was to ensure ‘plasma bonding’ of these materials with the same performance as cured PDMS by finding the right protocol and process parameters.

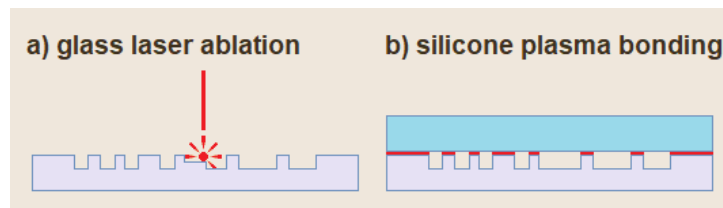


Figure 2. Glass laser ablation

2. Concept of the test device

Devices, characterized by a simple geometry reported in Figure 3, were made to test under pressure the bonding between glass layers and silicone layers. Three separated channels are engraved on the glass layer. The central one, the inlet channel, is sealed at one end and has a pocket at the other end. The two lateral channels are the drains, which are sealed at one end and open to the atmosphere at the other. The geometry dimensions are reported in Figure 4. The area 0.8 mm wide and 33 mm long, between the central channel with pressurized liquid and the lateral channels open to the outside, is analyzed to validate the tightness of the plasma bonding. A leak in this area is detected by the liquid coming out from the lateral channels.

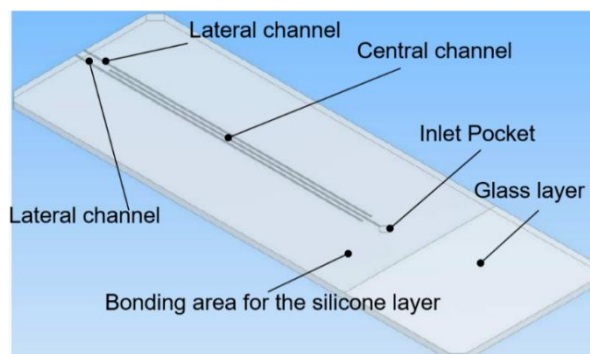


Figure 3. Concept of the microfluidic device

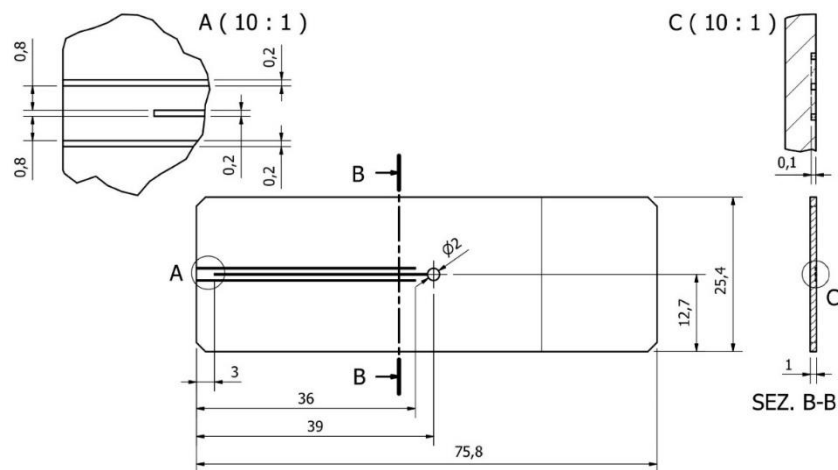


Figure 4. ISO technical drawing of the glass layer with dimensions in [mm]

A 3mm silicone layer is plasma bonded on the glass layer. A micro tube is connected to the central channel through the silicone layer, pierced on the pocket by a puncher. The thickness of the silicone layer ensures a secure connection between the test device and the tube.

The bonding tests were performed by filling the central channel with colored water under pressure through the tube. The pressure was increased step by step, to include the common field of application of microfluidic circuits. At each step the device was checked. If the bonding between the silicone layer and the glass layer was correct, the water remained sealed within the central channel. If the bonding was not correct, the water leaked from the lateral channels. This issue is discussed later in the paper.

3. Laser Ablation

The ultrashort laser systems opened new and unexpected possibilities in laser processing and micro-manufacturing such as laser processing in cold-ablation regime, with reduced heat affected zones and the processing of transparent materials such as glasses, ceramics, diamonds, polymers, and semiconductors thanks to multiphoton absorption [9]. We decided to test this technology for the realization of the channels in our test device using the third harmonic beamline of an EKSPLA Atlantic 5 picosecond laser. This source can produce pulses with a duration of about 10 ps with a repetition rate up to 1 MHz. In combination with a tight focus of about 10 μm it results in very high peak power, allowing sharp and fine engraving with limited glass heating and breaking.

The laser parameter, based on previous data collection on different test devices, were:

- 0,77 W measured power
- 355 nm wavelength
- 100 kHz repetition rate
- 300mm/s scan speed
- 20-50-75-100 number of passes
- 3 μm fill spacing of the engraving lines

The quality of the geometry obtained was analyzed measuring the dimensions of the channels and checking their shape by means of a confocal microscope Leica DMi 8. Scans were performed along the depth of the canal, with a step of 1 μm for the 20 laser passes, to reconstruct its shape, Figure 5.

The figure 6 shows the correlation found between the number of passes and the depth of the channel. The correlation is not linear beyond 50 passes, and the depth changes very little, probably for the same reasons that define the shape of the channel section. It should be noted that while the shape and depth of the channels are very important for the correct functioning of microfluidic circuits, they are much less so for the devices used to test under pressure the bonding between glass layers and silicone layers. Furthermore, the depth of the channels of normal microfluidic circuits is much less than 0.1mm and laser ablation is able to obtain channels with a very sharp section. All the samples used for pressure bonding tests were made with 20 laser passes, obtaining a channel depth of 0.1mm.

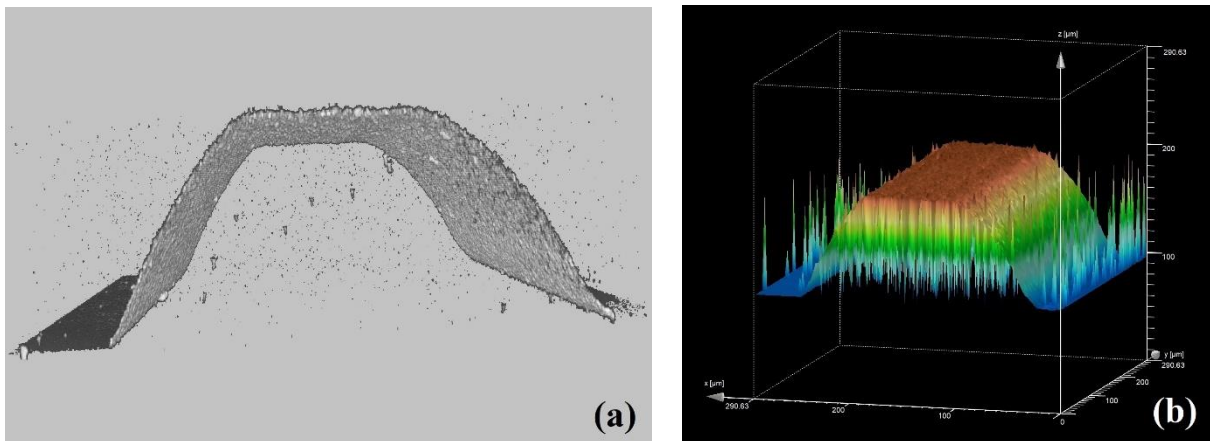


Figure 5. (a) Shape of a channel, (b) Dimensions of a channel. Laser passes 20. Channel depth 0.1mm. Factors such as depth / width ratio of the engraving, cone angle of the beam, and parallax errors inevitably lead to the U or V shape of the channel section [15].

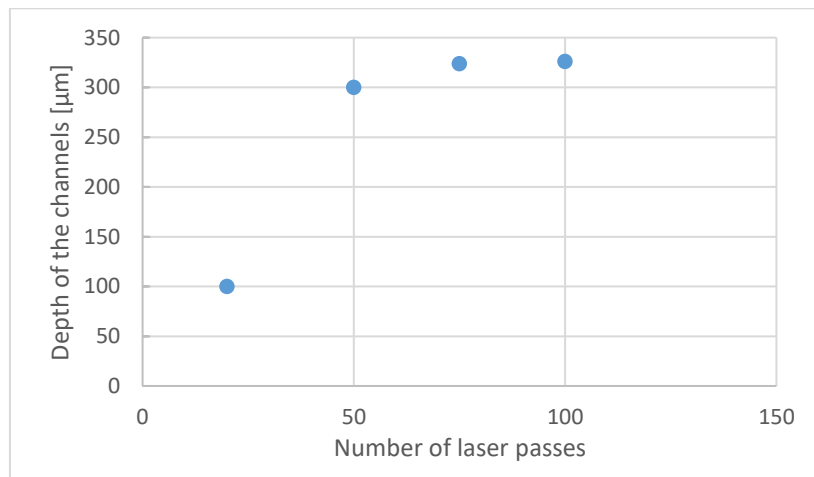


Figure 6. Correlation between the depth of the channels and the number of laser passes

4. Plasma Bonding

4.1. Bonding

Finding a bonding method that would not interfere with the normally biological fluids flowing within the microfluidic channels has been a major problem in microfluidic devices. The most popular and still most widely used method is 'plasma bonding'. This technology consists of activating surfaces through treatment inside a cold plasma machine, i.e., a type of plasma in which the electrons are not in thermodynamic equilibrium with the other gaseous species present, as they are characterized by a much higher temperature than the heavier species (ions and neutral species). The gasses normally used in microfluidic devices are air and oxygen at an absolute pressure of some tenths of mbar. Collisional processes involving 'hot' electrons and 'cold' gas molecules can give rise to dissociation reactions and the formation of radical species. Considering our case of bonding between silicone and glass through surface activation, the silicone end groups can be replaced by silane groups (SiOH) making the surface more hydrophilic and increasing its wettability. After plasma activation, the silicone is immediately brought into contact with the glass surface, which is itself plasma-treated and therefore also rich in surface Si-OH groups, to form through a condensation reaction a Si-O-Si bond at the interface between the two materials [16]. The covalent Si-O bond, being a very strong bond, thus ensures irreversible and effective bonding between the two materials. So, to make this process happen, it is easy to understand that specific materials are needed so that these steps described above can take place.

In our work, they were used three different materials for glass bonding, two different types of PDMS and one FDA silicone. They are all part of the elastomeric silicone family, also known as silicone rubbers or silicones, i.e. synthetic polymers with repeating siloxane groups $[\text{Si}(\text{CH}_3)_2\text{O}]_n$ unit along the backbone. PDMS is the most widely used material in microfluidics, due to its durability, gas permeability, chemical inertness and transparency that allows excellent optical access useful for experiments. For the experimental tests, they were used two different types of PDMS, the SSP-M823 from SSP Inc. commercially available in sheets of different thickness and the Dow Chemical's two-component Sylgard 184 kit to be cured in laboratory.

The last material is the L/SF silicone FDA from the SATI Group, produced with components that are included in the list of suitable products according to U.S. Food & Drug Administration, Code of Federal Regulations Title 21, Chapter 1, Subchapter B, Paragraph 177.2600. Like SSP-M823, the silicone FDA is commercially available in sheets of different thicknesses, and has technical and physical properties like PDMS, but not its transparency. Furthermore, it is not as expensive as PDMS.

4.2. First qualitative test of the bonding

Bonding was carried out using the Plasma Cleaner Smart Plasma 2 machine from Plasma Technology GmbH, Figure 7 with its data sheet reported in Table 1, which uses air as process gas.



Figure 7. Plasma Cleaner Smart Plasma 2 - Plasma Technology GmbH

Table 1. Plasma Cleaner Smart Plasma 2 – DATA SHEET.

	Description	Data
Inner dimension of the vacuum chamber	W x H x D	110 x 110 x 200 mm
Chamber volume		11.5 liters
Material used	Vacuum chamber	Stainless steel
	Electrode	Aluminum
Plasma generator	Frequency	20 – 50 kHz
	Power	Max. 80W
Vacuum pump (recommended)	Flow rate	5 m ³ /h
Operating pressure on the system		0.1 – 0.4 mbar
Pressure measurement		Pirani sensor
	Number of channels	1 (2 as option)
Process gas	Gas type	Air
	Primary pressure	Max, 0,5 bar
	Connections	6 mm hose connection

The tests were performed using laboratory glass slides and layers of the previously mentioned silicones. After foreplay tests, a precise procedure was established, which led to a correct bonding of the two interfaces. First, the samples were treated with an isopropanol solution and heated with hot air.

Subsequently, the two materials were placed in the plasma machine chamber, together but separated, and processed for the set time and power. At the end of the process, they were extracted, joined together using a couple of spring clamps and put back into the chamber for a second passage to stabilize the bonding. Based on the parameters found in the literature and after initial trials, it was decided to use the following combinations of time and power, at a chamber pressure set at 0.3 mbar. On a maximum power of 80W, 40%, 60%, and 100% were used for exposure times of 30, 60 or 120 seconds.

A qualitative assessment was assigned with figures ranging from 0 to 5, where 0 indicates no bonding and 5 a correct bonding on the whole surface – bonding strength equal to or greater than the material strength. The middle values 1, 2, 3 and 4 are proportional to the bonding strength and bonding area. This assessment was helpful in finding the optimal initial parameters for this process.

4.3. Parameters for optimal bonding

The results obtained are shown in Figure 8, where in the three graphs, one for each type of silicone, the x-axis shows the exposure time, the y-axis the power, and the color map indicates the bonding assessment values.

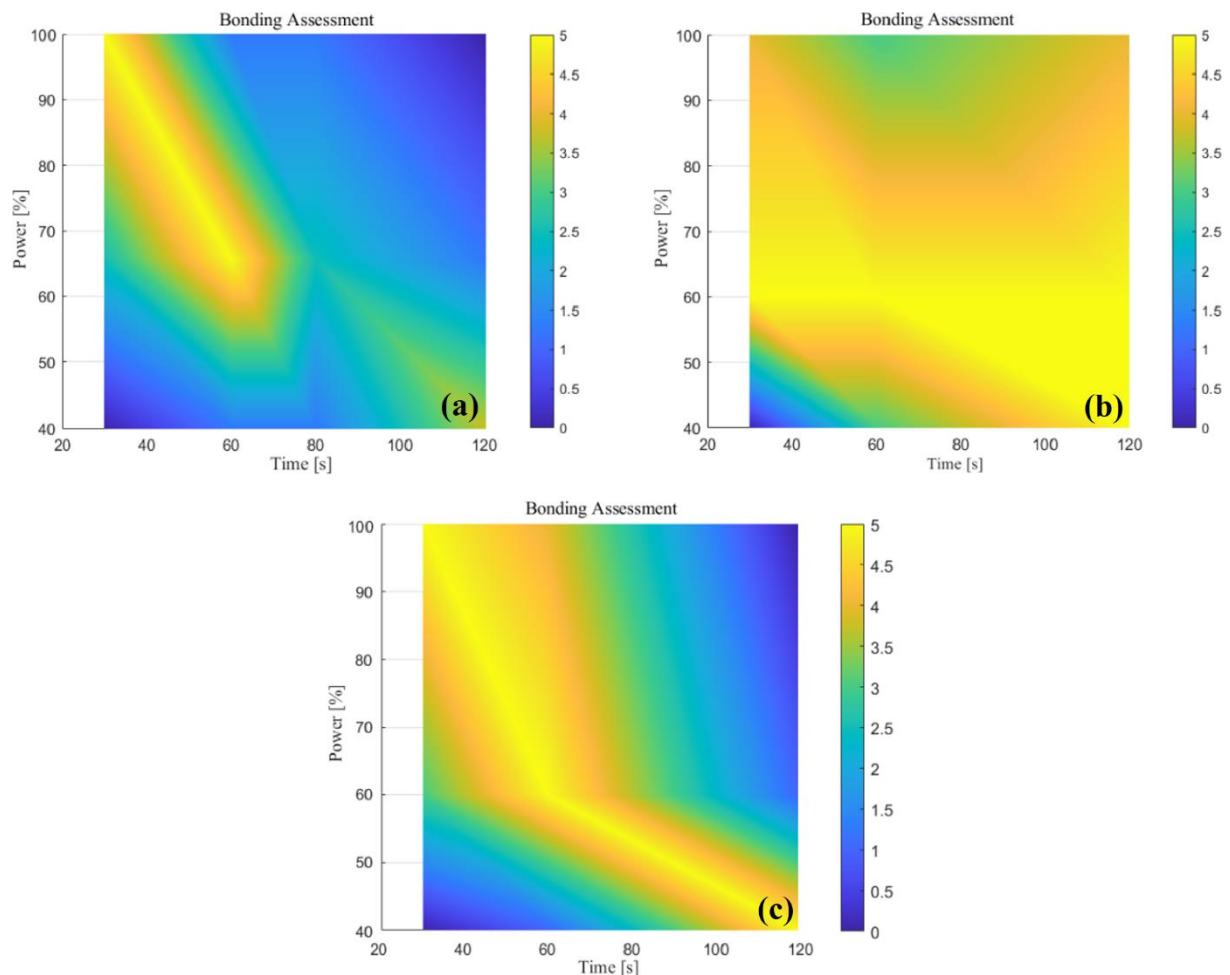


Figure 8. Bonding assessment graphs: (a) SSP-M823, (b) Sylgard 184, (c) L/SF silicone FDA.

In all three graphs, the optimal parameters are positioned approximately on a diagonal. This suggests that the two parameters do not independently affect the bonding. However, to obtain the best bonding, to the growth of one must correspond the reduction of the other, and vice versa. PDMS SSP-M823 has a very narrow area of optimal parameters, PDMS Sylgard 184 has a large area, and L/SF silicone FDA has an intermediate area, which improves with high power levels.

A narrow area of optimal parameters results in large deviations in bonding for small changes in parameters, so we discarded the SSP-M823. For subsequent tests, we chose L/SF silicone FDA because it has a sufficient area of optimal parameters, albeit smaller than Sylgard 184, is less expensive, has fewer work steps and a shorter lead time. The optimal parameters for this material are as follows: 100% (80W) / 30s, 60% (48W) / 60s, and 40% (32W) / 90s.

5. Bonding Tests on FDA silicone

The test procedures used to validate the bonding are not standardized and there are not common procedures, as far as the authors know. We therefore decided, based on our experience, to create our own procedure that could simulate most of the needs of microfluidic circuits.

5.1. Simplified Microchip

Simplified microchips, Figure 4, were made with laser ablated glass and plasma bonded with 3mm FDA silicone layer. They were used three different plasma bonding power levels (40, 60, and 100%) and three different plasma times (40, 60, and 90s). Batches of three simplified microchips were bonded with each pair of power level and time, for a total of 27 samples.

In the central channel of the simplified microchip, without outlets to the outside, it was introduced under pressure water colored with a dye (Ponceau S - Sigma Aldrich). The two lateral channels, which have an outlet to the outside, were used to detect any leaks of the central channel.

5.2. First Stage Pressure Tests

We created a hydraulic head pressure generator, Figure 9, with four different pressure levels, 200, 400, 800, and 1600mm H₂O ($2.0 \cdot 10^3$, $3.9 \cdot 10^3$, $7.8 \cdot 10^3$, and $1.6 \cdot 10^4$ Pa). Liquid Flows Tygon Tubing Microfluidic Connection Kit (Darwin Microfluidics) was used for connections, 60mL BD Biocoat Luer-Lock Disposable Syringe (Darwin Microfluidics) as water reservoir, and a graduated aluminum rod to support the reservoir.

Each sample was tested at increasing pressure levels, with a 60s stand-by at each level. If a leak was detected during the 60s stand-by, the test was terminated, and the sample was assigned the lower pressure level as exceeded.

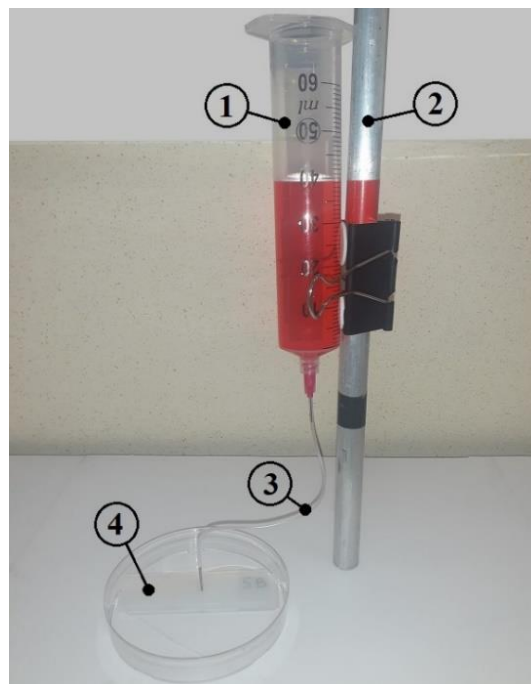


Figure 9. Hydraulic head pressure generator, 200mm test: (1) Water reservoir; (2) Graduated aluminum rod; (3) Micro tube; (4) Test device.

5.3. Second Stage Pressure Tests

We created an air pressure generator, Figure 10, with three different pressure levels, $3.0 \cdot 10^4$, $6.0 \cdot 10^4$, and $1.0 \cdot 10^5$ Pa. They were used a manual mechanical pump to generate a maximum pressure of 6 bar, a 5m long $\phi 12$ mm polyurethane air hose as a high-pressure air reservoir, an air restrictor with valve and 0-1 bar pressure gauge to reduce the high pressure at the various output pressure levels, and a small reservoir as an air-water interface.

Each sample that passed the first step was tested at the new pressure levels, with a 60s stand-by at each level. If a leak was detected during the 60s stand-by, the test was terminated, and the sample was assigned the lower pressure level as exceeded.

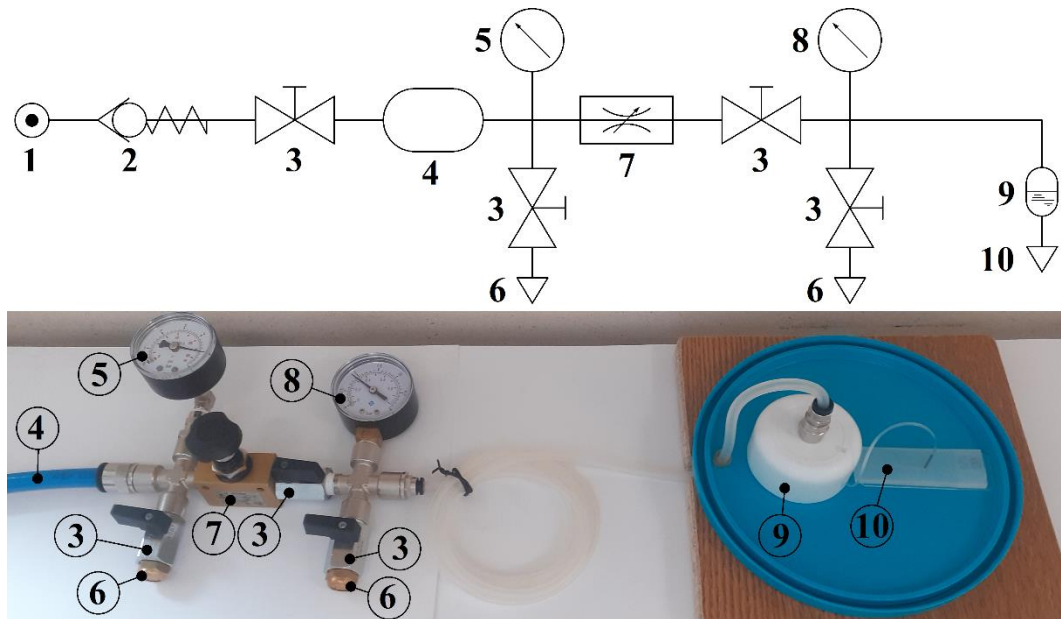


Figure 10. Air pressure generator: (1) Air inlet from the manual pump; (2) Non return valve; (3) Manual valve; (4) Air hose as high-pressure air reservoir; (5) 0-6 bar manometer; (6) Vent; (7) Air restrictor; (8) 0-1 bar manometer; (9) Air-water reservoir; (10) Water output to the test device.

Figure 11 shows the pressure test values, calculated as the average of the results of the three samples of each batch. Each batch is associated with a different pair of power level and time. In Figure 12 the same values of the pressure tests are shown in graphic form through a color map.

		Bonding pressure [Pa]		
Time [s]	90	Batch 7 6.7E+04	Batch 8 6.7E+04	Batch 9 7.2E+03
	60	Batch 4 6.7E+04	Batch 5 8.7E+04	Batch 6 8.7E+04
	40	Batch 1 6.5E+02	Batch 2 6.7E+04	Batch 3 8.7E+04
		40	60	100
		Power [%]		

Figure 11. Numerical values of pressure tests

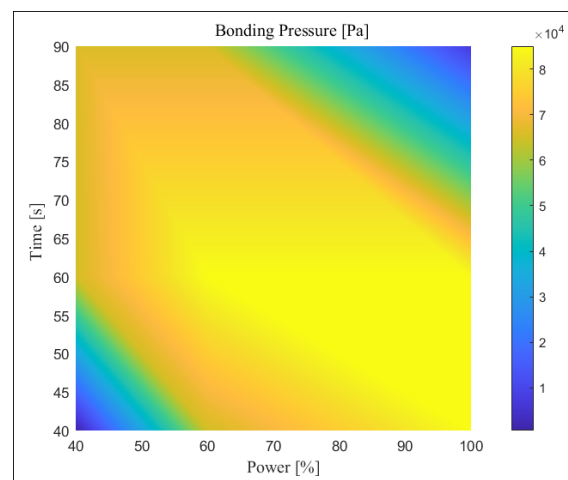


Figure 12. Graphic values of pressure tests

The results of the pressure tests shown in Figure 12 agree with the results of the qualitative tests of the first bonding with FDA silicone, Figure 8.c. Again, the results suggest that the two parameters, power level and the exposure time, do not independently affect the bonding. However, to obtain the best bonding, to the growth of one must correspond the reduction of the other, and vice versa. The area of optimal parameters is large enough, allowing variations of the optimal parameters without compromising the quality of FDA silicone bonding.

Furthermore, the pressure of $1.0 \cdot 10^5$ Pa (1 bar), withstood by the bonding of many samples in this area of optimal parameters, is very high and exceeds any need required by normal microfluidic circuits. It is conceivable that by restricting the area of optimal parameters, FDA silicone can withstand higher pressures in the case of special applications.

6. Conclusions

The work presented here was aimed to the realization of a microfluidic device consisting of a layer of glass sealed with a layer of silicone. The device channels were produced on the glass layer by laser ablation using an ultrashort laser source. A commercial silicone layer was joined to the glass layer using the plasma bonding process. Although these two technologies are not new in the scientific literature, their use for the production of the microfluidic devices has only been explored to some extent. It is very challenging to find clear indications for the laser ablation manufacturing of the channels on the glass layer, in particular regarding the setting of the laser parameters and number of passes with respect to the channel geometry, the surface finish and also the control of the shape of the channels section. At the moment, a qualitative analysis is being conducted and is described in the paper, gathering enough information to highlight the critical issues and to guide the next step work, which will focus on making a more complex geometry using different laser settings. The plasma bonding of the glass and silicone layer was thoroughly investigated, using several silicone layers, testing different plasma machines, polishing and pre-heating the surfaces and setting different parameters. These data are not readily available in literature and have been reported in this article to describe the work done, the criticality of the process and to guide other researchers who need to go through the same process and test other materials. Finally, two different tests were described for the validation of the bonding and the assessment of its quality, showing then the results obtained and the effectiveness of the process.

The next activities of the research project will be:

- design of a two-flow micromixer with herringbones, a standard microfluidic circuit, with the same technology shown in this work,
- CFD analyses in order to improve the geometry to find the best mixing performance,
- construction of test samples, according to the design and the indications of CFD analyses,
- experimental tests to evaluate the mixing performance of the samples, comparing it with that of existing devices, and validate the device design and CFD analysis,
- experimental tests to assess how the manufacturing quality of the channels affects the fluid dynamic conditions and the mixing.

7. References

- [1] Salerno E, Orlandi G, Ongaro C, d'Adamo A, Ruffini A, Carnevale G, Zardin B, Bertacchini J and Angeli D 2022 Liquid flow in scaffold derived from natural source: experimental observations and biological outcome *Regenerative Biomaterials* **9** rbac034
- [2] Malloggi F 2016 *Soft Matter at Aqueous Interfaces*, ed Peter Lang and Yi Liu (Switzerland: Springer Cham) chapter 16 p 515
- [3] Bharat B 2010 *Handbook of Nanotechnology* (Springer Heidelberg) pp 503-507
- [4] Roselli P 2017 *Corso di Laurea Magistrale in Ingegneria Biomedica: Validazione sperimentale di dispositivi microfluidici provvisti di strutture idrodinamiche di tipo Herringbone per la cattura cellulare via adesione selettiva* 42-43
- [5] Tien J, Nelson C M, and Chen C S 2002 *Fabrication of aligned microstructures with a single elastomeric stamp* **99** 1758-62
- [6] Mukhopadhyay R 2007 When PDMS isn't the best *Analytical Chemistry*, vol 79(9) pp 3248-53

- [7] Wlodarczyk K L, Hand D P and Maroto-Valer M M 2019 *Maskless, rapid manufacturing of glass microfluidic devices using a picosecond pulsed laser*
- [8] He F, Liao Y, Lin J, Song J, Qiao L, Cheng Y and Sugioka K 2014 *Femtosecond Laser Fabrication of Monolithically Integrated Microfluidic Sensors in Glass* 8-15
- [9] Wei Y, Wang T, Wang Y, Ho Y-P and Ho H-P 2022 *Rapid Prototyping of Parafilm® -based analytical microfluidic devices using laser ablation and thermal fusion bonding* 3-4
- [10] Orazi L, Romoli L, Schmidt M and Li L 2021 Ultrafast laser manufacturing: from physics to industrial applications *CIRP Annals* vol 70(2) pp 543-566
- [11] Wlodarczyk K et al 2018 Rapid Laser Manufacturing of Microfluidic Devices from Glass Substrates *Micromachines* vol 9(8) p 409
- [12] Butkutė A and Jonušauskas L 2021 3D Manufacturing of Glass Microstructures Using Femtosecond Laser *Micromachines* vol 12(5) p 499.
- [13] Wlodarczyk K L, Hand D P and Maroto-Valer M M 2019 *Maskless, rapid manufacturing of glass microfluidic devices using a picosecond pulsed laser* **9** 20215
- [14] Orazi L et al. 2022 *Ultrafast laser micromanufacturing of microfluidic devices. Proceedings of V CIRP Conf. on Biomanufacturing* (in press)
- [15] Al-Halhouli A, Al-Faqheri W, Alhamarneh B, Hecht L and Dietzel A 2018 *Spiral microchannel with trapezoidal cross section fabricated by femtosecond laser ablation in glass for the inertial separation of microparticles*
- [16] Borók A, Laboda K and Bonyár 2021 A PDMS bonding technologies for microfluidic applications: A review *Biosensors* (Elsevier Science) vol 11 pp 15-16

8. Acknowledgements

This work has been supported by the project " Epigenetic Regulation of Nuclear Inositides in Bone Marrow Microenvironment and MDS/AML Progression: New Targets, Therapy and Drugs" funded by the MIUR Progetti di Ricerca di Rilevante Interesse Nazionale (PRIN)- Bando 2017 Prot. 2017RKWNJT.